SAND2018-1886C

Uncertainty Quantification Framework for Wind Turbine Wake Measurements with a Scanning Lidar

Thomas Herges[1], David Maniaci[1], and Brian Naughton[1]
Sandia National Laboratories, Albuquerque, NM, 87185

Sandia National Laboratories and the National Renewable Energy Laboratory conducted a field campaign at the Scaled Wind Farm Technology (SWiFT) Facility using a customized scanning lidar from the Technical University of Denmark. The results from this field campaign were used to assess the predictive capability of computational models to capture wake dissipation and wake trajectory downstream of a wind turbine. The present work used large-eddy simulations of the wind turbine wake and a virtual SpinnerLidar to quantify the uncertainty of wind turbine wake position due to the line-of-sight sampling and probe volume averaging effects of the lidar. The LES simulations were of the SWiFT wind turbine at both a 0° and 30° yaw offset with a stable inflow. The wake position extracted from the simulated lidar sampling had an uncertainty of 2.8 m and 5.8 m as compared to the wake position extracted from the full velocity field with 0° and 30° yaw offset, respectively. The larger uncertainty in calculated wake position of the 30° yaw offset case was due to the increased angle of the wake position relative to the axial flow direction and the resulting decrease in the line-of-sight velocity relative the axial velocity.

I. Introduction

A team of researchers at Sandia National Laboratories (SNL) and the National Renewable Energy Laboratory (NREL) conducted a field experiment at the DOE Scaled Wind Farm Technology (SWiFT) Facility [1-4] to investigate the use of wind turbine yaw control to direct wakes [5-7]. Data collected as part of the multi-month field campaign will be used to improve both the high-fidelity wind plant simulation software, as well as demonstrate control concepts to facilitate future wind industry controls technology development for reducing wake losses. One of the most challenging requirements of the experimental campaign was to capture detailed characteristics of the wake produced by the upwind turbine. To confirm the model predictions, long-term continuous measurements of the wake velocity profile downwind of the turbine were needed to obtain a statistical sample. To address this challenge, the team partnered with the Technical University of Denmark (DTU) Wind Energy Department to leverage their wake measurement expertise and their custom-built SpinnerLidar, which is well suited to the temporal and spatial resolution required for the SWiFT experiment [8-10].

One of the primary objectives of the experiment was to collect experimental data to validate wind plant computational tools with respect to the response of the wake center, the wake velocity deficit strength, and the wake shape for a series of wind turbine yaw offsets during a range of atmospheric conditions. The methodology for this validation effort was based on a formal Verification and Validation (V&V) framework, which was used for the development and execution of coordinated modeling and experimental programs to assess the predictive capability of computational models of complex systems through focused, well structured, and formal processes [11]. This work focuses primarily on the experimental elements of the V&V method, specifically on the uncertainty quantification (UQ) of wake measurements obtained with the SpinnerLidar. Uncertainty quantification of these measurements will eventually be used to estimate the confidence intervals on the wake position and velocity deficit strength true values. These confidence intervals will be used to establish an acceptable range of experimental predictions for a set of inflow boundary conditions.

Lidar measurements present a unique challenge when quantifying uncertainty for validation of computational simulations. Lidars measure the line-of-sight (v_{los}) component of the wind velocity within a probe volume rather than the axial velocity at a regular grid point in space, which is the value commonly extracted from simulations. The lidar also scans through the flowfield along surfaces that are not necessarily orthogonal to the simulation coordinate system. Thus, comparisons of what and where the lidar measures with quantities of interest that are easily extracted from simulations have a higher uncertainty when compared to lidar-analogous quantities of interest extracted with a simulated lidar. The simulated lidar essentially smooths the simulated data with a temporal and spatial filter specific to the lidar properties.

[1] Senior Member of the Technical Staff, Wind Energy Technologies Department

The present work uses Large Eddy Scale (LES) simulations to quantify the uncertainty in wake position due to comparing what the lidar measures with what is typically extracted from simulations. The NREL-developed Simulator for Wind Farm Applications (SOWFA) code was used to simulate the wake of the SWiFT turbine. A virtual DTU SpinnerLidar was implemented to sample the simulated wake creating the equivalent spatial and temporal filtering as the lidar measurements [6]. The same wake tracking algorithm was applied to both the instantaneous streamwise velocity at points in a perpendicular plane as to the virtual lidar probe-volume averaged line-of-sight velocities along a curved surface to quantify the uncertainty of the wake position from these different velocity fields.

This work contributes a piece to the overall UQ of the SpinnerLidar measurements of wind turbine wakes at the SWiFT facility. Future work will assess the UQ of additional quantities of interest such as wake shape, position, and velocity deficit. This framework will include the uncertainty of wake quantities of interest using the propagation of many sources of uncertainty in comparing SpinnerLidar measurements to independent simulations. These sources include (1) scanning through a temporally changing flow field, (2) line-of-sight sampling of the laser beam in a complex, three-dimensional flowfield that was not always aligned with the axial flow direction, (3) probe volume spatial averaging, (4) uncertainty in the measurement location, and (5) processing of the velocity data to the necessary quantities of interest. This paper focuses on quantifying the impact of items 1 – 3 on wake position using the comparison of LES simulated velocity fields with different spatial and temporal filtering effects caused by the lidar.

II. Experimental Configuration

Sandia National Laboratories operates the Scaled Wind Farm Technology (SWiFT) facility located in Lubbock, Texas. The baseline site instrumentation includes three research wind turbines (WTG) and two meteorological towers (MET) as shown in Fig. 1.

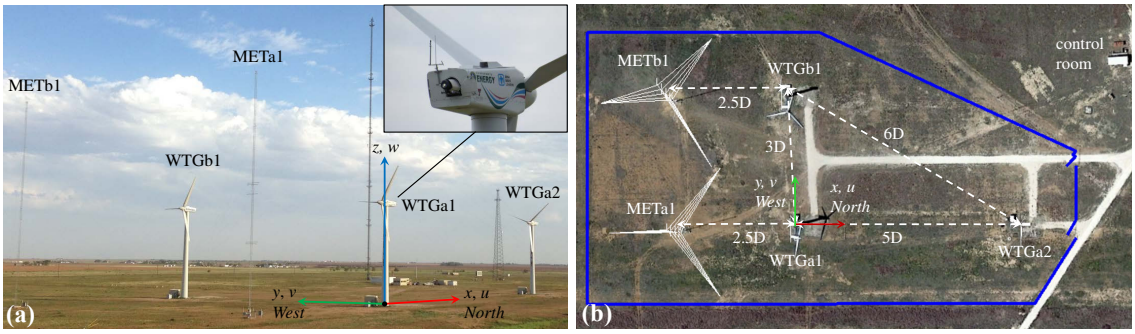

Figure 1. SWiFT site layout and coordinate system with the DTU SpinnerLidar installed in WTGa1 including a top view of the facility layout [1].

The layout of the SWiFT facility is seen from an overhead view in Fig. 1. The met tower and the two turbines used in this campaign (METa1, WTGa1, and WTGa2) are all aligned with the predominant wind direction at the site, 180 degrees (north is 0 degrees). This configuration allows measurement of the atmospheric inflow with the met tower and measurement of the wake of the WTGa1 turbine using the nacelle-mounted DTU SpinnerLidar. The SWiFT turbines are highly-modified, variable speed, variable collective pitch Vestas V27 machines with a hub height of 32.1 meters, a rotor diameter of 27 meters, and a maximum power output of 192 kW [1]. The meteorological towers are 59 m tall with a suite of atmospheric sensors as described in Ref. [3]. The entire site is on a fiber optic data acquisition and control network and each WTG and MET are individually synchronized to GPS.

The SpinnerLidar was mounted as shown in Fig. 1 to point out of the rear of the upwind SWiFT turbine nacelle, to be optimally positioned to capture the full wind turbine wake up to five rotor diameters downstream (D = 27 m). The lidar was configured to scan a rosette as shown in Figs. 2b and 3 at each of 5 rotor diameter distances downstream. Each rosette pattern of approximately 984 data points takes 2 second to complete and another 2 seconds to refocus to each sequential measurement plane downstream [3]. The lidar captured this wake data as the turbine operated under a variety of yaw offsets with respect to the predominant inflow direction (+25° to -12°) and under various atmospheric conditions characterized by wind speed, temperature profile, turbulence intensity, veer and shear. This combination of conditions was designed to test the model's ability to predict the wake reaction to a range of perturbations. Rotor loads and loads distribution will be derived from blade root strain (flap, fore-aft, and torsion), tower top deflection (fore-aft and side-side), tower strain, and thrust; a weighted combination of these measurements will be used along with the rotor azimuth location to derive the thrust, power, and load distribution across the rotor disc.

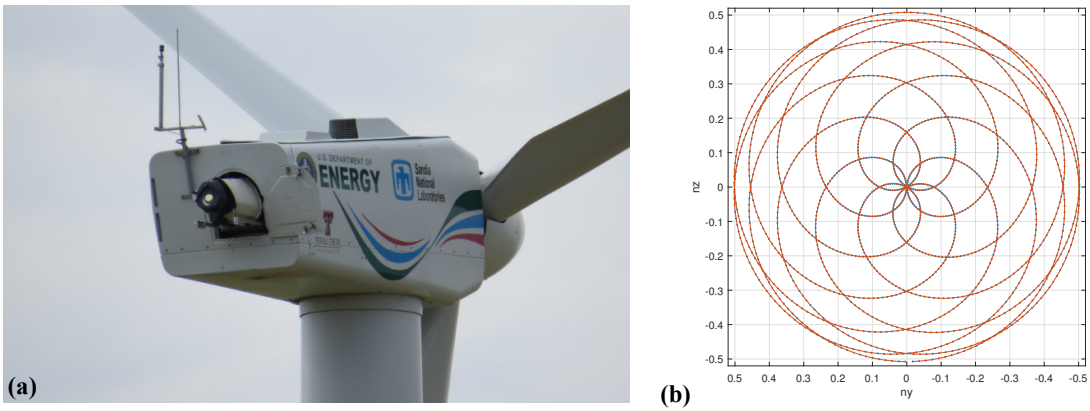

Figure 2. (a) A photo of the DTU SpinnerLidar installed in the turbine nacelle of one of the SWiFT site turbines, configured to measure the wake, and (b) calibrated DTU SpinnerLidar scan points in normalized lidar coordinates [3].

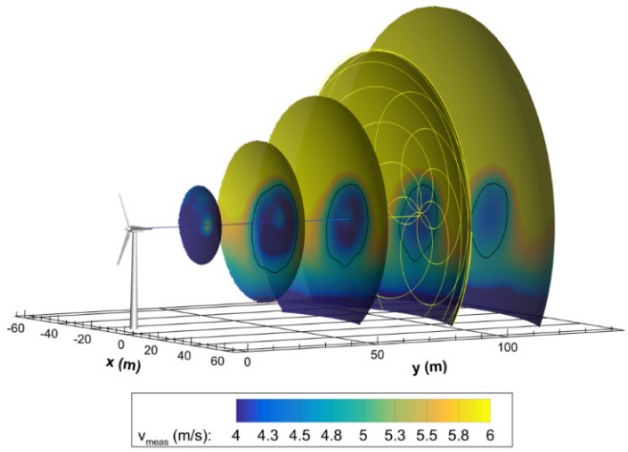

Figure 3. A screen capture from an animation (https://vimeo.com/162440208) depicting the SpinnerLidar scanning pattern at the SWiFT site overlaid on line-of sight (LOS) speed profiles extracted from virtual lidar simulations.

A. Wake Tracking Method

Wake tracking is an important quantity of interest for assessing wake steering as a control technology. Wake steering controllers intentionally misalign the wind turbine yaw heading with the wind direction, creating a prescribed yaw offset, that deflects the downstream wake. One goal of the wake steering field test at the SWiFT site was to evaluate the wake deflection corresponding to a distribution of yaw offsets (+25° to -12°). A number of processing steps were required to extract the wake position from the DTU SpinnerLidar line-of-sight measurements. First, the SpinnerLidar line-of-sight quality assurance and quality control (QA/QC) method removed data points that have a low level of laser signal return relative to the noise threshold as well as points contaminated with laser signal returns from stationary objects due to the introduction of slight object movement from the motion of the laser scan pattern. Second, the location of the measurements in the lidar coordinate system were scaled from an initial normalized frame (Fig. 2 b, which was calibrated in Ref. [4]) using the average focus distance over the scan. The actual focus distance at each measurement point can fluctuate as high as ± 2 m. This fluctuation was relatively small when compared to the probe volume length of the lidar (see Ref. [3]), resulting in a minimal change in the corresponding velocity measurement [12, 13]. The orientation and position of the lidar relative to the ground and nacelle was determined using total station theodolite (TST) measurements [4]. The lidar roll and pitch angles were measured by a calibrated 3-axis accelerometer [4], and applied to the data to create the lidar coordinate system.

A bicubic, smoothing-surface fit was used to interpolate the irregular scan pattern to a regular grid. Next, the wake tracking algorithm was implemented on the line-of-sight velocity regular grid. In the first wake tracking step, the inflow atmospheric boundary layer velocity was subtracted from the measured downstream line-of-sight

velocity, revealing any velocity deficit region. The atmospheric boundary layer velocity was estimated as a power law fit of the un-waked edges of the downstream velocity scan. Second, the velocity deficit region from the wind turbine was identified, and the velocity deficit threshold was iteratively determined to match the constraint of an area threshold. In this case, the area threshold was set to match the rotor area. The area threshold allows the wake tracking method to be robust for a variety of inflow and yaw offset conditions. However, it does not properly capture the expansion of the wake downstream. The wake center was then calculated from the weighted centroid of the velocity deficit within the area of the wake. Finally, the measurement points and wake position in the lidar coordinate system were transformed to the wind direction coordinate system using rotational coordinate transformations and the angle of the lidar relative to the rotor plane (lidar angle), the wind turbine yaw heading angle, and the wind direction angle measured from the hub-height sonic anemometer.

B. DTU SpinnerLidar Simulations

Figure 3 is a screen capture from an animation (https://vimeo.com/162440208) that was created from a virtual lidar model and LES SOWFA [8] CFD simulation of the SWiFT site and turbines. The video depicts in real-time and scale, one of the SWiFT turbines operating while the DTU SpinnerLidar scans a rosette pattern at five distances downstream (1 – 5 rotor diameters). The contour surfaces at each scanning distance represent the average line-of-site speed interpolated from the SpinnerLidar virtual model interrogation of the simulation, providing an estimation of the resolution of data that can be expected during the experiment. The black irregular shape at each distance represents the output of the wake tracking method to determine the center of the wake produced by the turbine.

The LES simulations of the SWiFT site V27 wake sampled with a virtual DTU SpinnerLidar [6] offer a method of assessing the uncertainty between wake tracking in an instantaneous regularized plane, easily extracted from simulations, and wake tracking from the spatially and temporally filtered line-of-sight velocity data. The atmospheric conditions used in the simulation are listed in Table 1. The simulations are slightly different from the actual measurements acquired in the field campaign. In the simulations, the SpinnerLidar sampled 625 points in 2 seconds. The wind turbine had yaw offsets of 0°, ±15°, and ±30°, and the lidar was angled at ±10° relative to the rotor plane during the ±15° and ±30° wind turbine yaw offsets. The full details of the SpinnerLidar simulations are provided in Ref. [6].

Table 1: Summary of atmospheric inflow conditions used in SOWFA simulations [6].

Case	surface roughness (m)	surface temp. flux (K-m/s)	hub-height wind speed/direction (m/s/degrees)	hub-height shear exponent	hub-height turbulence intensity, TI (%)	Bulk Richardson Number	Obukhov length, L (m)
Stable	0.01	-0.03	6.5/180	0.29	8.5	0.147	34.5

Figure 4 shows a comparison with actual DTU SpinnerLidar measurements and a simulation sampled with the virtual SpinnerLidar for similar inflow conditions and yaw offset at a downstream distance of 2.5 D. In general the velocity deficit of the wind turbine wake appears to be higher in the actual measurements than the simulations, and the fluctuations in wake position also appear to be higher in the measurements.

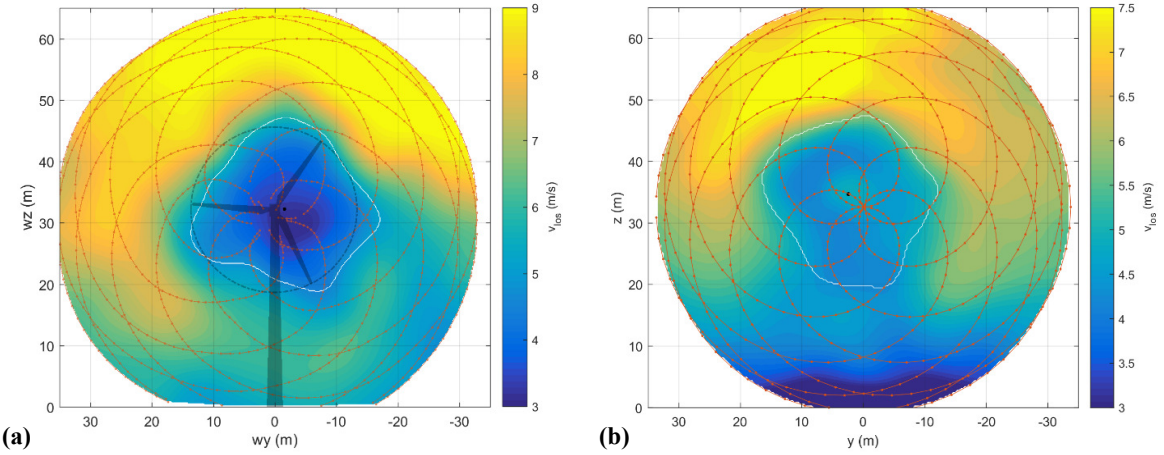

(a) (b)

Figure 4. DTU SpinnerLidar (a) full field measurement comparison with (b) simulated lidar sampling measurements.

III. Results

From LES simulations, high resolution streamwise velocity at points in a perpendicular plane are typically obtained, while a scanning lidar acquires probe-volume averaged line-of-sight velocities along a curved surface. It is important to understand the impact of uncertainty quantification resulting from the difference between what is simply extracted from measurements and simulations when comparing quantities of interest for verification and validation purposes.

Figure 5 shows a comparison of simulated velocities in the wind turbine wake region, at 5D downstream, sampled using various methods. These velocity fields were generated using the inflow conditions listed in Table 1 with a 0° wind turbine yaw offset and 0° lidar angle. The instantaneous axial velocity component, u_{inst}, in a plane perpendicular to the flow is presented in Fig. 5a. Figure 5b displays the same axial velocity field as Fig. 5a interpolated to the SpinnerLidar scan pattern and then interpolated back to regular grid points using the same bicubic smoothing surface fit that was used in the processing of the SpinnerLidar measurements (labeled as u_{scan}). The virtual SpinnerLidar sampled velocity field without the spatial filtering of the lidar probe volume is shown in Fig. 5c ($v_{los\ no\ pv}$), while the addition of the probe volume spatial averaging is presented in Fig. 5d (v_{los}). The v_{los} measurements match how the SpinnerLidar samples the flowfield. Each part of Fig. 5 shows a different effect of the spatial and temporal filtering from lidar measurements. Figure 5b compared to Fig 5a reveals the cross plane spatial averaging of the lidar scan pattern and interpolation method. The temporal filtering of the lidar sampling in addition to the effect of the line-of-sight velocity versus streamwise velocity is shown by comparing Figs. 5b and 5c, while Fig. 5d reveals the additional spatial filtering along the laser vector by including the probe volume averaging. However, even with the varying degrees of spatial and temporal filtering, the wake position extracted from each velocity field was very similar. Figure 6 displays the same velocity fields for the same stable inflow, but with a 30° wind turbine yaw offset and a -10° lidar angle. Again, the extracted wake center was similar between the flow fields even though the wake shape was not perfectly preserved.

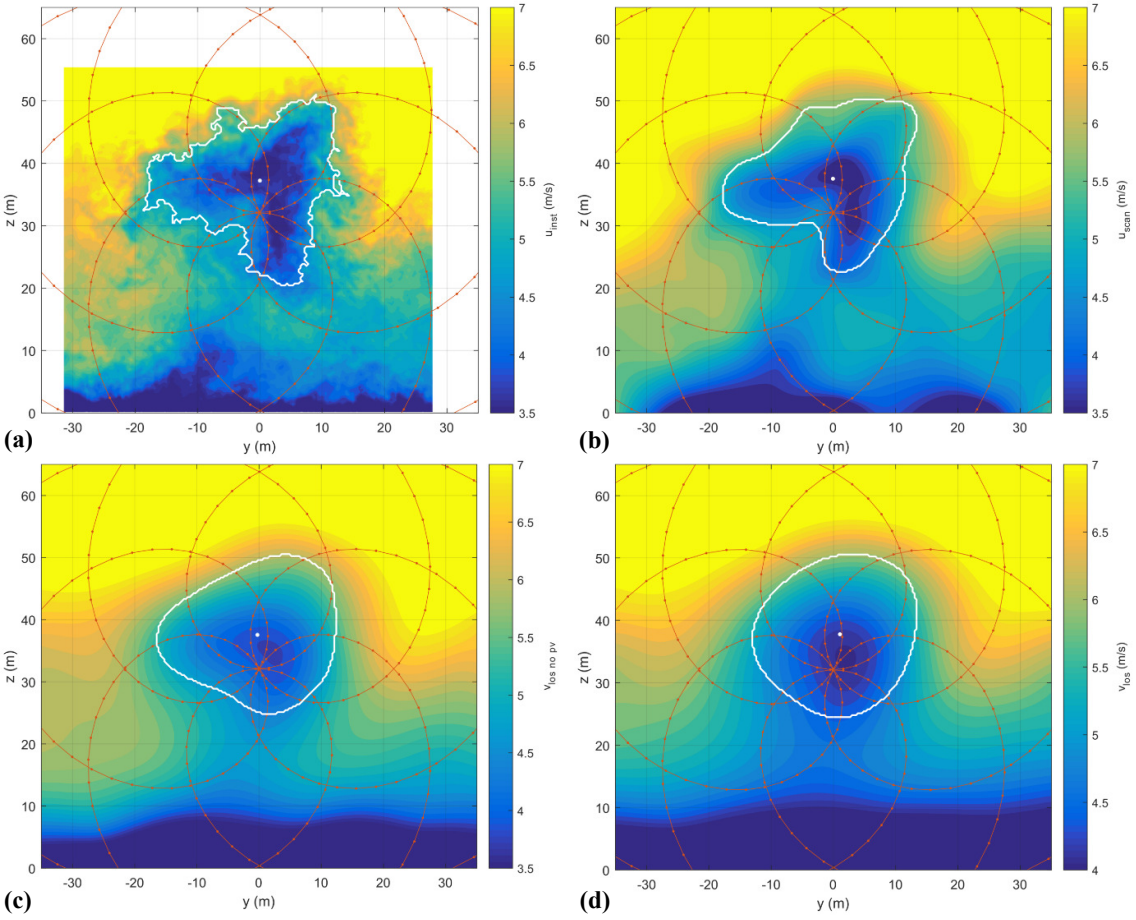

Figure 5. Stable inflow (Table 1) with 0° wind turbine yaw offset and lidar angle velocity fields with various levels of lidar filtering: (a) u_{inst} instantaneous axial velocity, (b) u_{scan} instantaneous axial velocity sampled by lidar scan pattern, (c) $v_{los\ no\ pv}$ lidar line-of-sight sampled flow field without probe volume averaging, and (d) v_{los} lidar sampled flow field with probe volume averaging.

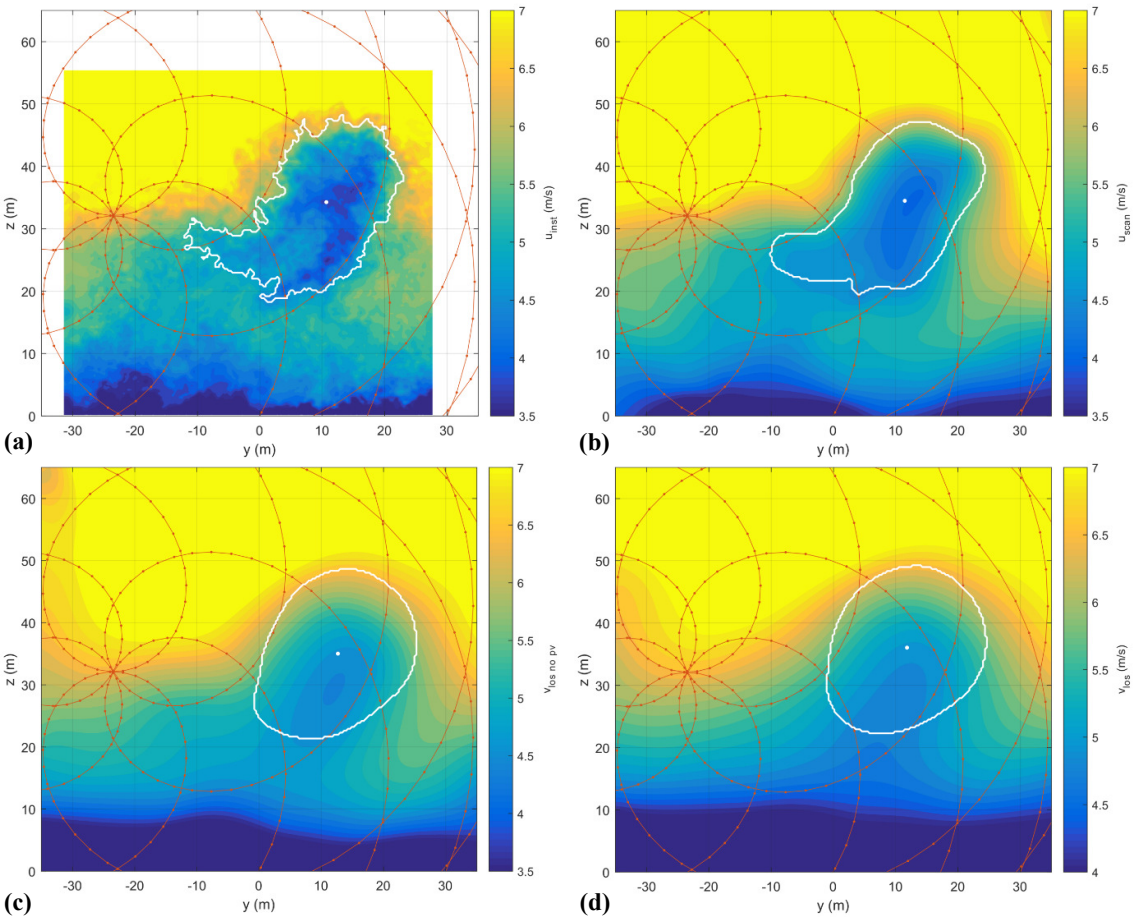

Figure 6. Stable inflow (Table 1) with 30° wind turbine yaw offset and -10° lidar angle velocity fields with various levels of lidar filtering: (a) u_{inst} instantaneous axial velocity, (b) u_{scan} instantons axial velocity sampled by lidar scan pattern, (c) $v_{los\ no\ pv}$ lidar line-of-sight sampled flow field without probe volume averaging, and (d) v_{los} lidar sampled flow field with probe volume averaging.

The wake tracking algorithm was applied to 298 and 299 time steps for the different velocity fields in Figs. 5 and 6, respectively. The wake center was compared between each of the sampled velocity fields at multiple distances downstream (2 D, 3 D, 4 D, and 5 D). The object was to improve insight into the effects of probe volume averaging, line-of-sight velocity versus streamwise velocity, and the impact of the interpolation scheme on wake tracking. The lateral wake positions in the u_{inst}, u_{scan}, and $v_{los\ no\ pv}$ velocity fields were compared with the lateral wake position found in the v_{los} velocity field, since the v_{los} velocity field is most like the SpinnerLidar measurements. Figure 7 displays the distributions of the distance between wake centers for a 0° (left column) and 30° (right column) yaw offset at 5 D downstream. The first, second, and third rows in Fig. 7 compares the distance in wake center (in the *y*-*z* plane) between u_{inst} and v_{los}, u_{scan} and v_{los}, and $v_{los\ no\ pv}$ and v_{los}, respectively.

The results show that with a 0° yaw offset, the wake was located within 2.8 m (95% confidence interval) from the v_{los} sampled wake regardless of the level of filtering on the velocity field, and the distribution in distances between wake centers were also very similar. The 2.8 m uncertainty in the v_{los} wake position as compared to u_{inst}, corresponds to a 1.2° uncertainty in the lidar position angle in the nacelle. The largest variation in wake position occurs between v_{los} and u_{inst} with a 30° yaw offset and -10° lidar angle. The wake position is bound by a 95% confidence interval at 5.8 m, or a corresponding lidar angle uncertainty of 2.5°. The increased yaw misalignment with the inflow direction and non-zero lidar angle enlarge the bounds on the distribution of distances between the v_{los} and u_{inst} wake centers. To determine if the increased wake position uncertainty was due to the inflow misalignment or lidar angle, two additional configurations were analyzed where the yaw offset remained 0°, while the lidar angle increased to -10° and -20°. The results from this comparison are summarized in Table 2 with an increase in the uncertainty of wake position to 3.3 m and 3.1 m for the -10° and -20° lidar angles, respectively. The increase in wake position uncertainty was minimal as compared to the 30° yaw offset case.

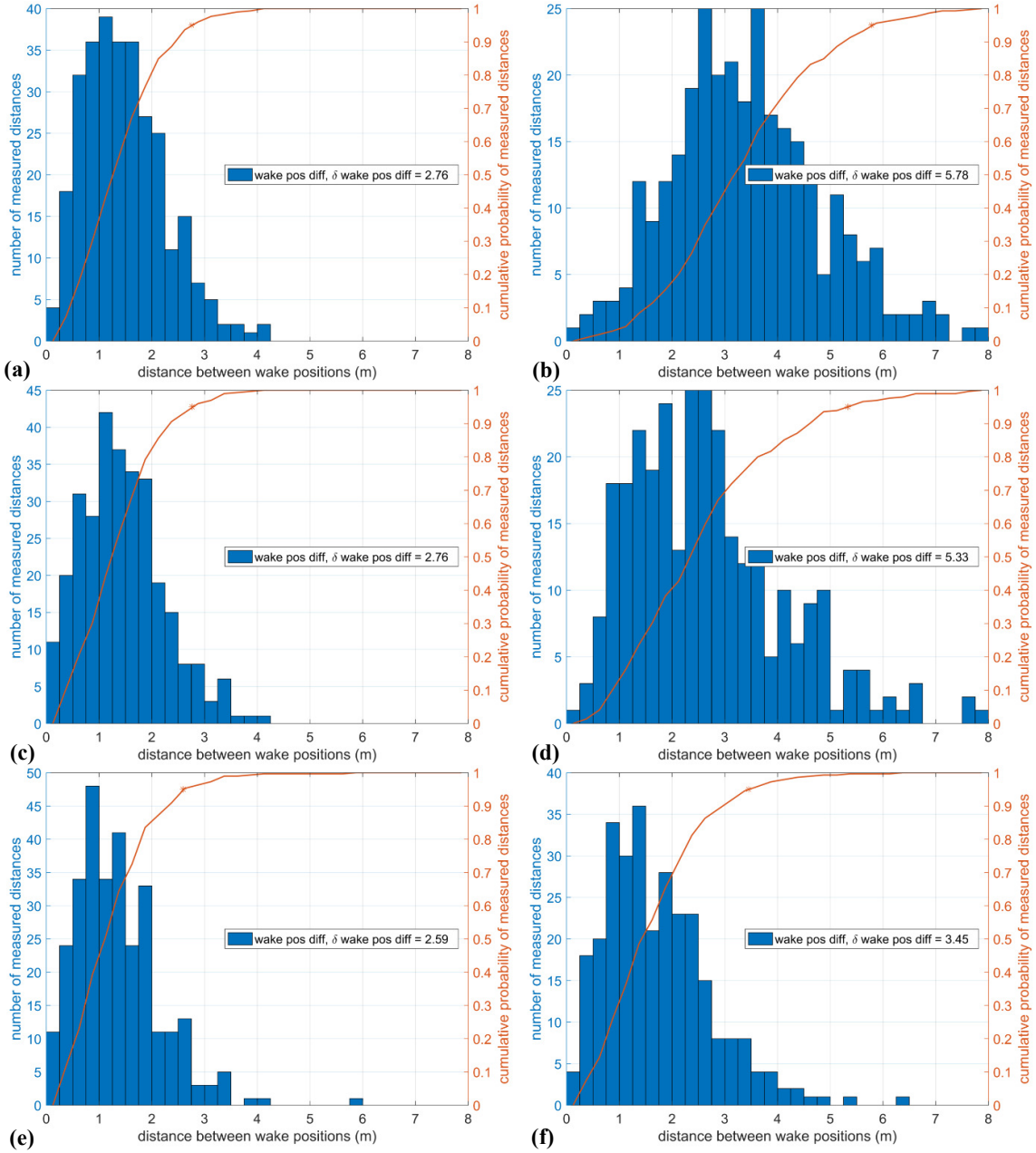

Figure 7. Distributions of distance between wake centers for a 0° (left column) and 30° (right column) yaw offset at 5 D downstream: (a) u_{inst} and v_{los} 0° yaw, 0° lidar angle, (b) u_{inst} and v_{los} 30° yaw, -10° lidar angle, (c) u_{scan} and v_{los} 0° yaw, 0° lidar angle, (d) u_{scan} and v_{los} 30° yaw, -10° lidar angle, (e) $v_{los\ no\ pv}$ and v_{los} 0° yaw, 0° lidar angle, and (f) $v_{los\ no\ pv}$ and v_{los} 30° yaw, -10° lidar angle.

The 0° yaw offset wind turbine resulted in an average wake deflection of 2.8 m from the wind turbine centerline in both the u_{inst} and v_{los} velocity fields, while the 30° yaw offset resulted in an average 9.5 m and 11.2 m deflection in the u_{inst} and v_{los} velocity fields, respectively. This result indicates that the increased uncertainty in wake position between the u_{inst} and v_{los} velocity fields is likely because the lidar line-of-sight vector that captures the wake position in the 30° yaw offset case was not as aligned with the axial flow direction as in the 0° yaw offset case. This means that the magnitude of v_{los} relative to u_{inst} at the wake position decreases as the wake deflects away from the wind turbine centerline. The lidar line-of-sight vector at the wake position was still aligned with the axial flow direction during the increased lidar angle cases with 0° yaw offset since the wake was only deflected 2.8 m. The wake appeared in a different portion of the scan pattern during the large lidar-angle cases but the line-of-sight vector was still aligned with the inflow direction better than in the 30° yaw offset case. Since the wake tracking algorithm uses a velocity deficit threshold to find the wake position, the wake would artificially be located

further toward the edge of the v_{los} scan pattern as the wake moves away from the centerline of the turbine and lidar position for a given inflow direction. Figure 7f shows a lower wake position uncertainty than Figs 7b and 7d, helping to support the conclusion that the difference between the line-of-sight velocity and axial velocity skews the wake position as the wake moves away from the downstream centerline of the wind turbine and lidar positions.

The analysis of the results focused on the wake position uncertainty at 5D since that was the position of the downstream wind turbine at the SWiFT facility. The general trend of the wake position uncertainty at the different downstream positions was an increase in the uncertainty of the corresponding lidar angle at 2 D relative to at 5 D, and a reduced uncertainty in corresponding lidar angle at 3 D and 4 D for all the wind turbine yaw offset and lidar angle configurations.

Table 2: Wake position uncertainty between velocity fields for each wind turbine yaw offset and lidar angle configuration at 5 D downstream. The lidar angle uncertainty was calculated from the arctangent of the wake position uncertainty and lidar focus distance.

comparison	0° yaw, 0° lidar (m, °)	30° yaw, -10° lidar (m, °)	0° yaw, -10° lidar (m, °)	0° yaw, -20° lidar (m, °)
v_{los} - u_{inst}	2.76, 1.17	5.78, 2.45	3.33, 1.41	3.09, 1.31
v_{los} - u_{scan}	2.76, 1.17	5.33, 2.26	3.57, 1.51	3.81, 1.62
$v_{los} - v_{los\ no\ pv}$	2.60, 1.10	3.45, 1.46	2.88, 1.22	2.73, 1.56

IV. Conclusions

Lidar measurements present a unique challenge when quantifying uncertainty for validation of computational simulations. Lidars measure the line-of-sight (v_{los}) component of the wind velocity within a probe volume rather than the axial velocity at a regular grid point in space, which is the value commonly extracted from simulations. LES simulations of the SWiFT wind turbine wake, sampled with a virtual DTU SpinnerLidar, offered insight into the effects of the following sources of uncertainty on measured wake position: scanning through a temporally changing flow field, line-of-sight sampling rather than axial velocity measurements, and probe volume averaging. The LES simulations were of a wind turbine at both a 0° and 30° yaw offset with a stable inflow. The wake position extracted from the lidar sampled simulations had an uncertainty of 2.8 m and 5.8 m as compared to the wake position from a non-lidar sampled velocity field simulation with a 0° and 30 °wind turbine yaw offset, respectively. The 30° yaw offset had an increased uncertainty in the wake position due to the greater lateral deflection of the wake away from the wind turbine, resulting in an increased angle relative to the axial flow direction. This increased angle created a greater difference between the line-of-sight velocity and the axial velocity in the vicinity of the wake, skewing the calculated wake position away from the downstream centerline of the wind turbine and lidar positions. This analysis is a piece in an overall larger framework of Uncertainty Quantification of SpinnerLidar wake measurements at the SWiFT facility.

Acknowledgments

This work was supported by the U.S. Department of Energy under Contract No. DE-AC04-94AL85000 with Sandia National Laboratories, a multimission laboratory managed and operated by National Technology and Engineering Solutions of Sandia, LLC, a wholly owned subsidiary of Honeywell International, Inc., for the U.S. Department of Energy's National Nuclear Security Administration under contract DE-NA-0003525 with the National Renewable Energy Laboratory. Funding for the work was provided by the DOE Office of Energy Efficiency and Renewable Energy, Wind Energy Technologies Office as part of the Atmosphere to Electronics (A2e) research program. In addition to our DOE sponsors, the authors would like to acknowledge Jonathan Berg, Joshua Bryant for their help with supporting and running the SWiFT wind turbine and Torben Mikkelsen and Mikael Sjöholm from DTU for developing the DTU SpinnerLidar and helping to deploy it at the SWiFT site. The authors also thank the SWiFT support staff, David Mitchell, Miguel Hernandez, Kolton Foster, and David Martinez, Andrew Scholbrock and Donald Baker from the NREL for their support with the SpinnerLidar at SWiFT and the NREL colleagues working on the Wake Steering Experiment including Matt Churchfield who performed the SOWFA simulations that were analyzed in this work.

References

1. Berg, J., Bryant, J., LeBlanc, B., Maniaci, D. C., Naughton, B., Paquette, J. A., Resor, B. R., White, J., and Kroeker, D. "Scaled Wind Farm Technology Facility Overview," *32nd ASME Wind Energy Symposium*. American Institute of Aeronautics and Astronautics, 2014.
2. Kelley, C. L., and Ennis, B. L. "SWiFT Site Atmospheric Characterization," *SAND-2016-2016*. Sandia National Laboratories, 2016.
3. Herges, T. G., Maniaci, D. C., Naughton, B. T., Mikkelsen, T., and Sjöholm, M. "High resolution wind turbine wake measurements with a scanning lidar," *Journal of Physics: Conference Series* Vol. 854, No. 1, 2017.
   doi: 10.1088/1742-6596/854/1/012021
4. Herges, T. G., Maniaci, D. C., Naughton, B., Hansen, K., Sjöholm, M., Angelou, N., and Mikkelsen, T. "Scanning Lidar Spatial Calibration and Alignment Method for Wind Turbine Wake Characterization," *35th Wind Energy Symposium*. American Institute of Aeronautics and Astronautics, 2017.
5. Fleming, P., Gebraad, P. M. O., Lee, S., Wingerden, J.-W. v., Johnson, K., Churchfield, M., Michalakes, J., Spalart, P., and Moriarty, P. "Simulation comparison of wake mitigation control strategies for a two-turbine case," *Wind Energy* Vol. 18, No. 12, 2015, pp. 2135-2143.
   doi: 10.1002/we.1810
6. Churchfield, M., Wang, Q., Scholbrock, A., Herges, T., Mikkelsen, T., and Sjöholm, M. "Using High-Fidelity Computational Fluid Dynamics to Help Design a Wind Turbine Wake Measurement Experiment," *Journal of Physics: Conference Series* Vol. 753, No. 3, 2016, p. 032009.
7. Fleming, P., Churchfield, M., Scholbrock, A., Clifton, A., Schreck, S., Johnson, K., Wright, A., Gebraad, P., Annoni, J., Naughton, B., Berg, J., Herges, T., White, J., Mikkelsen, T., Sjöholm, M., and Angelou, N. "Detailed field test of yaw-based wake steering," *Journal of Physics: Conference Series* Vol. 753, No. 5, 2016, p. 052003.
8. Mikkelsen, T., Angelou, N., Hansen, K., Sjöholm, M., Harris, M., Slinger, C., Hadley, P., Scullion, R., Ellis, G., and Vives, G. "A spinner-integrated wind lidar for enhanced wind turbine control," *Wind Energy* Vol. 16, No. 4, 2013, pp. 625-643.
   doi: 10.1002/we.1564
9. Machefaux, E., Larsen, G. C., Troldborg, N., Hansen, K. S., Angelou, N., Mikkelsen, T., and Mann, J. "Investigation of wake interaction using full-scale lidar measurements and large eddy simulation," *Wind Energy* Vol. 19, No. 8, 2016, pp. 1535-1551.
   doi: 10.1002/we.1936
10. Sjöholm, M., Pedersen, A. T., Angelou, N., Abari, F. F., Mikkelsen, T. K., Harris, M., Slinger, C., and Kapp, S. "Full two-dimensional rotor plane inflow measurements by a spinner-integrated wind lidar," *European Wind Energy Association Conference*. 2013.
11. Hills, R. G., Maniaci, D. C., and Naughton, J. W. "V&V Framework," *SAND-2015-7455*. Sandia National Laboratories, 2015.

12. Angelou, N., Mann, J., Sjöholm, M., and Courtney, M. "Direct measurement of the spectral transfer function of a laser based anemometer," *Review of Scientific Instruments* Vol. 83, No. 3, 2012, p. 033111.
doi: 10.1063/1.3697728
13. Horváth, Z. L., and Bor, Z. "Focusing of truncated Gaussian beams," *Optics Communications* Vol. 222, No. 1–6, 2003, pp. 51-68.
doi: http://dx.doi.org/10.1016/S0030-4018(03)01562-1